

Fast Spin-Echo for Multiple Mouse Magnetic Resonance Phenotyping

Brian J. Nieman,* Nicholas A. Bock, Johnathan Bishop, John G. Sled, X. Josette Chen, and R. Mark Henkelman

High-resolution magnetic resonance imaging is emerging as a powerful tool for phenotyping mice in biologic studies of genetic expression, development, and disease progression. In several applications, notably random mutagenesis trials, large cohorts of mice must be examined for abnormalities that may occur in any part of the body. In the aim of establishing a protocol for imaging multiple mice simultaneously in a standardized high-throughput fashion, this study investigates variations of a three-dimensional fast spin-echo sequence that implements driven equilibrium, modified refocusing, and partial excitation pulses. Sequence variations are compared by simulated and experimental measurements in phantoms and mice. Results indicate that when using a short repetition time ($TR \leq T_1$) a sequence employing a partial excitation tip angle provides both improved signal and good T_2 contrast compared with standard fast spin-echo imaging. This sequence is used to simultaneously acquire four live mouse head images at 100 μm isotropic resolution with a scan time under 3 h at 7 T. *Magn Reson Med* 54:532–537, 2005. © 2005 Wiley-Liss, Inc.

Key words: MRI; mouse imaging; multiple mouse MRI; fast spin-echo; phenotypic

The mouse has become the experimental animal of choice in biomedical research for modeling human disease and development processes. Physiologic and genetic similarities to humans (1) in addition to an extensive set of techniques for genetic manipulation (2) has allowed mouse models to improve the understanding of human development and treatment of human diseases. However, significant challenges lie in the initial detection and subsequent monitoring of informative phenotypes and abnormalities. The difficulty of phenotype identification is exacerbated by the large numbers of mice needed in typical biologic studies. This is particularly true in large random mutagenesis trials, where thousands of unique mutant mice are generated each year (3) and aberrant phenotypes may be present in any part or system of the body or may be absent altogether. Rapid, yet thorough, phenotyping of each animal becomes paramount for efficient detection and analysis of mutations.

The soft tissue contrast available with MRI offers an excellent means of assessing structural and anatomic abnormalities. However, there are several challenges in modifying human clinical MRI practice to large-scale MR mouse phenotyping. First, MR imaging must keep pace with large-scale biologic studies without compromising image quality. This challenge is met by parallelizing image acquisitions with multiple mouse MRI (MMMRI) (4), which accommodates multiple samples with independent radiofrequency coils within a single gradient and magnet. This technique provides an essential increase in throughput, but the need for slower large-bore gradient sets that accommodate many mice is potentially a disadvantage when compared to smaller high-performance microimaging gradients with only single or very limited mouse capacity. Second, image resolution must be increased approximately 15-fold in each linear dimension beyond human images to provide equivalent fractional anatomy at the mouse scale. This resolution should be three-dimensional and isotropic—potentially over the entire animal—in order to allow viewing in arbitrary orientations and to allow unbiased, quantitative, and automated phenotype detection (5) in large-scale studies. Finally, if phenotyping is to be conducted in vivo, the imaging session must also be restricted to the time that a mouse—even one with compromised health—can be reliably anesthetized. Two to three hours is a long but reasonable upper limit on scan time when using isoflurane gas anesthetic (6), allowing for handling and preparation. This study addresses the procedures for acquiring high-resolution images in this time-frame within the context of high-throughput MMMRI.

Image acquisition in the clinical environment has been greatly facilitated by the introduction of the pulse sequence “rapid acquisition with relaxation enhancement” (7), more commonly called fast spin-echo (FSE) or turbo spin-echo, due to its increased rate of data collection. FSE has the additional benefits of being insensitive to susceptibility differences and inherently T_2 -weighted; both desirable traits in animal imaging systems operating at high field strengths where susceptibility effects are increased and heavily T_2 -weighted images generally provide greater contrast. However, at higher field strengths T_2 relaxation times are shorter and T_1 relaxation times are longer, meaning fewer echoes can be acquired per excitation and a longer delay is needed between excitations for recovery. This reduces the efficiency of standard T_2 -weighted FSE image acquisitions and limits the resolution that can be achieved. For this reason, we have investigated possible modifications of the FSE pulse sequence so as to optimize image quality within the time available for mouse phenotyping. In particular, we investigated the possibility of

Department of Medical Biophysics, University of Toronto, Mouse Imaging Centre, Hospital for Sick Children, Toronto, Ontario, Canada.

Grant sponsor: Canada Foundation for Innovation/Ontario Innovation Trust; Grant sponsor: Ontario Research and Development Challenge Fund; Grant sponsor: National Institutes of Health; Grant sponsor: Burroughs Wellcome Fund.

*Correspondence to: Brian J. Nieman, Mouse Imaging Centre, Hospital for Sick Children, 555 University Avenue, Toronto, Ontario M5G 1X8, Canada. E-mail: brian.nieman@sw.ca

Received 8 September 2004; revised 23 March 2005; accepted 23 March 2005.

DOI 10.1002/mrm.20590

Published online 5 August 2005 in Wiley InterScience (www.interscience.wiley.com).

© 2005 Wiley-Liss, Inc.

reduced repetition time ($TR \leq T_1$) acquisition strategies that maintain good T_2 -weighted image contrast.

In this paper, four FSE sequence variants are considered, each managing available magnetization in a different manner. For reference purposes the first sequence is the standard FSE with a 90° excitation and 180° refocusing pulses. The second sequence, here referred to as driven equilibrium FSE, attempts to recover transverse magnetization with driven equilibrium pulses at the end of the FSE echo train (8,9). The third sequence, modified refocusing FSE, reduces the tip angle of refocusing pulses to less than 180° and provides larger stimulated echoes (10,11). The final sequence, partial excitation FSE, maintains 180° refocusing pulses for an even number of echoes but uses an excitation tip angle less than 90° in order to conserve longitudinal magnetization; this is analogous to Ernst small angle excitations in gradient-echo imaging protocols. Each of these sequences is considered through simulations as well as experiments in phantoms and fixed mice. The most promising sequence is also shown to acquire excellent three-dimensional images in live mice.

METHODS

The expected signal level from each sequence in several tissues of the mouse body was first considered theoretically. Simulations were performed by numerically evaluating normalized magnetization signal components in the longitudinal and transverse directions, with the latter divided into clockwise and counterclockwise rotating components (12). The sequence model consisted of a series of rotations corresponding to radiofrequency pulses (assumed to be instantaneous) or time delays. Relaxation was incorporated during time delays by recovery or decay as dictated respectively by the relaxation times T_1 and T_2 .

A 3D FSE sequence was developed for a Varian INOVA console (Varian NMR Instruments, Palo Alto, CA, USA) with a 7.0-T magnet (Magnex Scientific, Oxford, UK). The system is equipped with a 29-cm inner bore diameter gradient set (Tesla Engineering Ltd., Storrington, Sussex, UK) with 120 mT/m maximum amplitude and 870 μ s rise time. Successful sequence implementation required analysis and compensation of eddy currents along all gradient axes.

Comparison of simulation and experiment in a phantom provides a means of verifying sequence functionality. A phantom was made using 1% agar with CuSO_4 and NaCl concentrations of 0.5 and 1.4 mM, respectively. Longitudinal and transverse relaxation times were measured to be $T_1 = 1890 \pm 40$ ms and $T_2 = 137 \pm 3$ ms using a 2D spin-echo sequence with varying repetition and echo time. A two-dimensional profile of the phantom was then collected with each FSE sequence and the signal levels (normalized to the standard FSE sequence) were plotted against simulation. In the case of the partial excitation, replacement of simple square 180° refocusing pulses with composite refocusing pulses (of the form $90^\circ_x - 180^\circ_y - 90^\circ_x$) was beneficial in preserving signal. This composite pulse was expected to improve inversion of longitudinal magnetization in the presence of B_1 inhomogeneities (13). These composite pulses had little or no effect in the other sequences or in fixed mouse experiments so were only im-

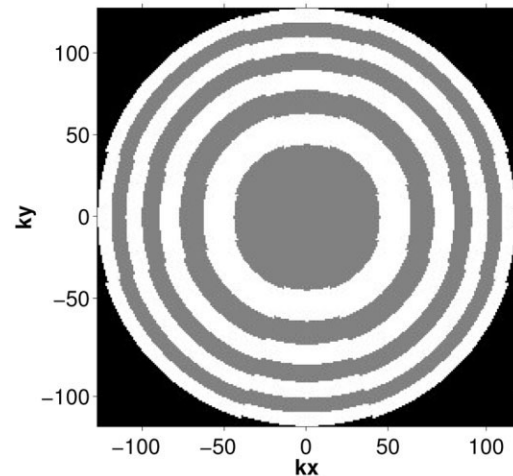


FIG. 1. Division of the two-dimensional 256×256 phase encode matrix into eight groupings. Black regions are not collected. Alternating gray and white regions represent eight groups that can be assigned to individual echoes in the echo train ($ETL = 8$) according to the desired contrast.

plemented for the phantom experiment. The unremarkable signal improvement in fixed mice is likely due to the limited performance of this composite pulse in the presence of B_0 inhomogeneity (14,15). More sophisticated pulse design for both inversion and refocusing in the presence of B_1 and B_0 inhomogeneities (14–16) is likely to show more noticeable effects in fixed and live mice, but was not considered further in the present experiments.

In order to compare images within a single specimen using the different sequences, a fixed mouse was prepared. Briefly, a mouse was anesthetized and then an IV catheter (0.62 mm diameter) and needle were guided by high-frequency ultrasound (Vevo 660, VisualSonics, Inc., Toronto, Ontario, Canada) to puncture the left ventricle. Fixation proceeded by perfusion of a saline and heparin solution followed by 10% buffered formalin phosphate (Fisher Scientific, Nepean, Ontario, Canada). The protocol was identical to the more detailed account in Zhou et al. (17) but without any contrast agent. Each FSE sequence was used to acquire a three-dimensional image using parameters $TE/TR = 14/800$ ms, echo train length $ETL = 8$, two averages, field of view $120 \times 30 \times 30$ mm, and matrix size $1024 \times 256 \times 256$. All sequences were acquired using a cylindrical k -space acquisition as shown in Fig. 1. In this scheme, only phase encode values lying on cartesian grid points of k -space within a specified radius are collected, resulting in a scan time reduction of 22%. Each phase encode grid point was grouped according to its distance from the center of k -space; ETL groups of an equal number of points were then individually assigned to echoes in the echo train. Within each grouping, phase encode points were collected by quadrant in a raster fashion, starting with the smallest phase encodes in the first phase encode dimension and proceeding to the largest. In the fixed mouse images, zeroth order k -space lines were collected on the second echo yielding an effective echo time $TE_{\text{eff}} = 28$ ms.

Live mice were imaged using the partial excitation sequence. In these experiments, four mice were imaged si-

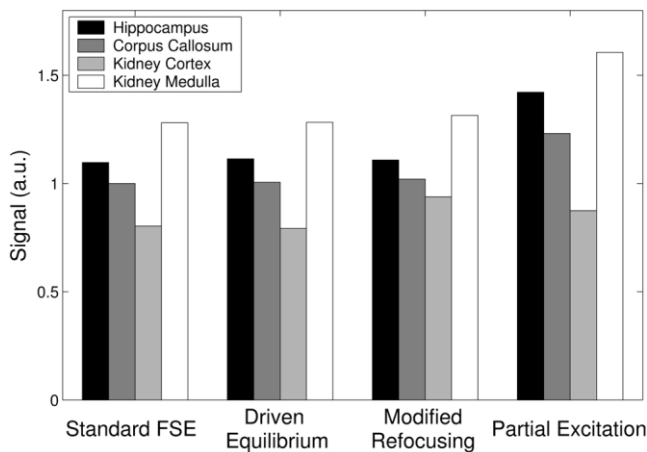


FIG. 2. Simulated signal results for four mouse tissues. Timing parameters include TR = 800 ms, echo spacing 14 ms, $TE_{\text{eff}} = 28$ ms, and ETL = 8. Tip angle details for each sequence are: standard FSE $90^\circ_x(180^\circ_y)^{\text{ETL}}$, driven equilibrium $90^\circ_x(180^\circ_y)^{\text{ETL}} + 190^\circ_{-x}$, modified refocusing FSE $90^\circ_x150^\circ_y(120^\circ_y)^{\text{ETL}} - 1$, partial excitation FSE $50^\circ_x(180^\circ_y)^{\text{ETL}}$.

multaneously using MMMRI with each mouse in a separate RF coil. Anesthesia was induced in the mice using vaporized isoflurane (Baxter Corp., Toronto, Ontario, Canada) at 4% concentration and then maintained for the duration of imaging at 0.8 to 1.0% concentration. The hardware for mouse handling as well as delivery and scavenging of anesthesia for multiple mice is described in detail elsewhere (18). Images were acquired with $TE/TR = 12/900$ ms, $TE_{\text{eff}} = 36$ ms, ETL = 8, two averages, field of view $40 \times 24 \times 24$ mm, and matrix size $400 \times 240 \times 240$ for an imaging time of 2 h 50 min. The excitation tip angle was set to 40° .

Reconstruction of three-dimensional images was performed with echo amplitude correction as described by Busse et al. (9). For the smaller in vivo data sets reconstruction was performed using standard MATLAB software (v 6.5.0 release 13, The MathWorks, Inc., Natick, MA, USA). The larger fixed mouse data sets were first processed for echo amplitude correction with MATLAB and then reconstructed using in-house software written for an SGI Origin 2000 with 32 CPUs and 32 gigabytes of RAM (Silicon Graphics, Mountain View, CA, USA).

All animal protocols were approved by the Hospital for Sick Children Animal Care Committee.

RESULTS

Calculated signals for four selected tissues of the mouse body are shown in Fig. 2 using the tissue properties provided in Table 1. The largest increase in signal level is observed using the partial excitation sequence for all tissues except the kidney cortex, where the modified refocusing FSE produces a larger signal. At even shorter TR values than shown here, the signal advantage of the partial excitation FSE becomes more pronounced. A notable increase in signal difference between the tissues consistent with an improved T_2 weighting is also present for the partial excitation sequence compared to the other sequences. This

Table 1
Tissue Properties Used in Simulation Results

Tissue	T_1 (ms) at 7 T	T_2 (ms) at 7 T	Relative proton density
Hippocampus	1767 ¹⁵	41 ¹⁵	0.66 ¹⁷
Corpus callosum	1503 ¹⁵	37 ¹⁵	0.56 ¹⁷
Kidney cortex	1035 ¹⁶	18 ¹⁶	0.76 ¹⁸
Kidney medulla	1593 ¹⁶	35 ¹⁶	0.79 ¹⁸

contrast improvement is strongly affected by the excitation tip angle; an excitation at the Ernst angle produces maximum signal, but further reducing the tip angle improves T_2 contrast at the expense of signal.

Figure 3 shows a comparison of simulation and experimental data in the agar phantom. Good agreement between the data is present for all sequences, with a somewhat reduced experimental signal in the partial excitation data. Separate experiments indicate that loss of longitudinal magnetization during the 180° pulses accounts for this loss in experimental signal intensity. This loss of longitudinal magnetization over the course of multiple 180° pulses is due to imperfect inversion with both B_1 and B_0 inhomogeneity (23,24).

Figure 4 displays regions of images of a fixed mouse for each of the sequence variations and a long TR FSE reference. Each of the four short TR sequence variations had approximately equivalent overall SNR, with significant local increases apparent in the partial excitation sequence. The long TR reference FSE has approximately twice the SNR of the other sequences. The contrast in the partial excitation sequence is much improved compared to the other sequence variations and mimics that of the long TR reference scan. Improvements are most noticeable in regions of vasculature and in the heart chambers where contrast-to-noise ratio increased threefold.

The partial excitation FSE sequence was also implemented with live mice. Figure 5 shows images from four three-dimensional data sets collected simultaneously in the mouse brain with $100\text{-}\mu\text{m}$ isotropic resolution. Figure

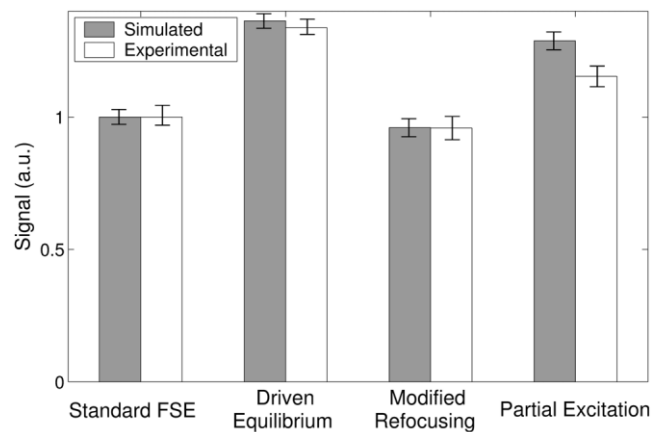


FIG. 3. Simulated and experimental signal results in an agar phantom. Phantom relaxation properties were measured to be $T_1 = 1890 \pm 40$ ms and $T_2 = 137 \pm 3$ ms. Timing parameters include TR = 800 ms, echo spacing 14 ms, $TE_{\text{eff}} = 28$ ms, and ETL = 8.

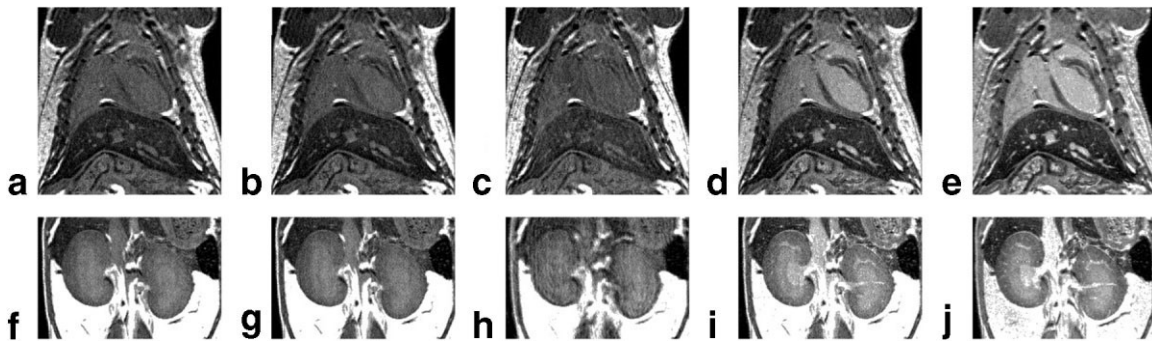


FIG. 4. Fixed mouse images. Cropped images of a 3D data set from the thorax (a–e) and kidneys (f–j). Images were collected using the standard FSE (a and f), driven equilibrium (b and g), modified refocusing FSE (c and h), partial excitation FSE (d and i), and standard FSE with long TR (e and j). The short TR sequences (a to d and f to i) had a total acquisition time of 170 min. The long TR reference sequence (e and j) had a total acquisition time of 645 min.

5b through d shows additional coronal, sagittal, and transverse slices from mouse 1. Image quality with respect to signal and contrast was similar in all mice with SNR ranging from 30 to 35. Likewise, artifact levels were comparable in all coil positions (mouse 1 in Fig. 4a was positioned at gradient isocenter with mice 2 and 4 offset vertically and mouse 3 offset horizontally in the bore). The successful implementation of the FSE in off-axis coil positions shows that MMMRI can be implemented with even more sophisticated, phase-sensitive pulse sequences without sacrifice in image quality.

DISCUSSION

The experiments here indicate that the partial excitation FSE sequence offers substantial improvement in the quality of multiple mouse images. From a spin management perspective, maintenance of some level of longitudinal

magnetization appears to be the best strategy of the alternatives presented. It reduces the recovery-induced T_1 weighting that otherwise degrades both signal and contrast in short TR sequences. The alternative strategies, recovering remaining transverse magnetization or storing more signal in stimulated echoes, are less effective. However, the trade-offs between these strategies is heavily dependent on T_1 and T_2 relaxation times and hence is inherently field dependent. For example, longer T_2 -relaxation times, such as the agar phantom in this study, greatly improve the performance of the driven equilibrium sequences. Indeed, driven equilibrium FSE scans have been successfully implemented at 1.5 T (9). It is expected that the gains we observe using partial excitation at 7.0 T will be less significant at lower field strengths but more significant at higher field strengths. Furthermore, these experiments anticipate MMMRI with a limited number of receivers and fourfold interleaving (4) so still have comparatively long TR. With

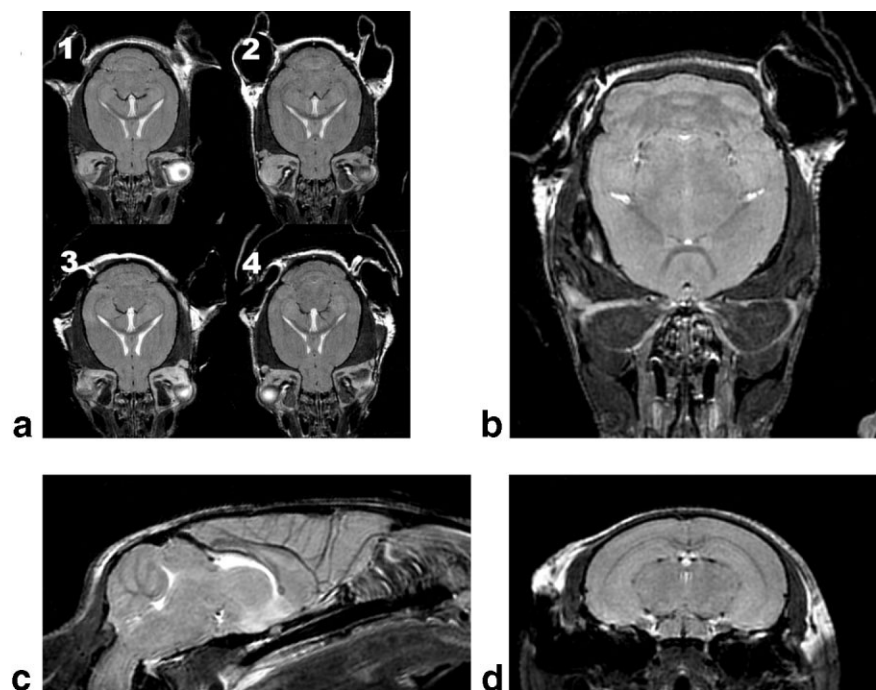


FIG. 5. Three-dimensional in vivo multiple mouse head scans. A coronal section from all four mice is shown in (a) with individual coronal, sagittal, and axial slices shown from mouse 1 in (b), (c), and (d), respectively. Images were collected with FOV $40 \times 24 \times 24$ mm and matrix $400 \times 240 \times 240$. Imaging time was 2 h 50 min. Images are rotated into a standard orientation.

individual receivers for each mouse, TR will be shortened considerably, making the preference for partial excitation even stronger.

The success of the partial excitation FSE depends critically on high-quality 180° refocusing pulses. Pulses that fail to invert all of the longitudinal magnetization cumulatively reduce signal over consecutive refocusing pulses and consequently degrade performance substantially. For this reason, a partial excitation FSE is not likely to be generally applicable in a clinical environment where the longer T_2 -relaxation times at lower field strengths permit more echo acquisitions. In addition, SAR considerations become critical in human imaging but are less restrictive in the anesthetized mouse where substantial external heating is required to maintain body temperature. Similar pulse quality limitations may exist in single mouse imaging where smaller specialized gradients run much faster and hence could obtain many more echoes in the same time period; in this scenario partial excitation would become increasingly difficult to manage in accordance with the increasing number of refocusing pulses. Nevertheless, the throughput gain achieved with multiple mouse MR (currently expected to achieve 19-fold on our system) is deemed critical for routine application in even modest scale biologic studies. In MMMRI at 7.0 T, with a large gradient set, we have shown significant image improvement with simple square 180° pulses using the partial excitation for T_2 -weighted FSE in the $TR \leq T_1$ timing regime.

As with human clinical studies, a major challenge in imaging live mice remains motion. Individual portions of the mouse, particularly the head, can be imaged through use of positioning techniques and local restraints (18) as we have shown. However, extension of these techniques to primary whole-body screening would require means of motion correction that are effective over the entire mouse. Problematically, the FSE is very sensitive to motion due to its extended echo train (25). Reducing the length of the echo train has been shown to reduce artifacts in human studies (26), but also reduces efficiency. It is possible that the partial excitation FSE could be used to recover some of this efficiency loss through the use of a reduced TR. Simple averaging likewise aids in reducing the magnitude of ghosts due to motion, especially in moving from a single acquisition to two or three acquisitions (27,28), but doesn't represent a complete solution. Some FSE motion artifacts have also been improved through gradient moment nulling (29). The most successful motion correction technique to date, prospective gating, has proven very successful in cardiac imaging of single mice (30,31) but clearly does not work for multiple mice. However, retrospective gating with k -space oversampling is effective and is currently in development at our laboratory for multiple mouse cardiac imaging. Similar techniques should extend to respiratory gating of whole-body images with the requisite oversampling enabled by the reduced TR of the partial excitation FSE. The development of such motion correction schemes will be critical in large-scale biologic multiple mouse MRI studies for investigation of the entire mouse body.

While technical improvements are ongoing, many studies and applications of high-throughput multiple mouse MRI are currently possible. Studies within the brain par-

ticularly stand to benefit from the improved T_2 weighting and acquisition efficiency of the partial excitation FSE. Such studies include in vivo longitudinal study of brain tumors and genetic neuronal phenotypes as well as screening of abnormal brain anatomy.

CONCLUSIONS

This study has demonstrated that modification of a standard FSE through use of partial excitation allows acquisition of T_2 -weighted mouse images with short repetition times ($TR \leq T_1$). This allows for high-resolution imaging within the time available for in vivo imaging. In combination with parallelization through MMMRI, this enables large-scale biologic studies to be performed in vivo, including anatomic phenotyping in either longitudinal development or screening investigations.

ACKNOWLEDGMENTS

Brian Nieman is the recipient of a Canada Graduate Scholarship. Mark Henkelman is the recipient of a Canada Research Chair in Imaging.

REFERENCES

1. Waterston RH, Lindblad-Toh K, Birney E, Rogers J, Abril JF, Agarwal P, Agarwala R, Ainscough R, Alexandersson M, An P, Antonarakis SE, Attwood J, Baertsch R, Bailey J, Barlow K, Beck S, Berry E, Birren B, Bloom T, Bork P, Botcherby M, Bray N, Brent MR, Brown DG, Brown SD, Bult C, Burton J, Butler J, Campbell RD, Carninci P, Cawley S, Chiaromonte F, Chinwalla AT, Church DM, Clamp M, Clee C, Collins FS, Cook LL, Copley RR, Coulson A, Couronne O, Cuff J, Curwen V, Cutts T, Daly M, David R, Davies J, Delehaunty KD, Deri J, Dermitzakis ET, Dewey C, Dickens NJ, Diekhans M, Dodge S, Dubchak I, Dunn DM, Eddy SR, Elnitski L, Emes RD, Esvara P, Eyraes E, Felsenfeld A, Fewell GA, Flicek P, Foley K, Frankel WN, Fulton LA, Fulton RS, Furey TS, Gage D, Gibbs RA, Glusman G, Gnerre S, Goldman N, Goodstadt L, Grafham D, Graves TA, Green ED, Gregory S, Guigo R, Guyer M, Hardison RC, Haussler D, Hayashizaki Y, Hillier LW, Hinrichs A, Hlavina W, Holzer T, Hsu F, Hua A, Hubbard T, Hunt A, Jackson I, Jaffe DB, Johnson LS, Jones M, Jones TA, Joy A, Kamal M, Karlsson EK, Karolchik D, Kasprzyk A, Kawai J, Keibler E, Kells C, Kent WJ, Kirby A, Kolbe DL, Korf I, Kucherlapati RS, Kulbokas EJ, Kulp D, Landers T, Leger JP, Leonard S, Letunic I, Levine R, Li J, Li M, Lloyd C, Lucas S, Ma B, Maglott DR, Mardis ER, Matthews L, Mauceli E, Mayer JH, McCarthy M, McCombie WR, McLaren S, McLay K, McPherson JD, Meldrum J, Meredith B, Mesirov JP, Miller W, Miner TL, Mongin E, Montgomery KT, Morgan M, Mott R, Mullikin JC, Muzny DM, Nash WE, Nelson JO, Nhan MN, Nicol R, Ning Z, Nussbaum C, O'Connor MJ, Okazaki Y, Oliver K, Larty EO, Pachter L, Parra G, Pepin KH, Peterson J, Pevzner P, Plumb R, Pohl CS, Poliakov A, Ponce TC, Ponting CP, Potter S, Quail M, Reymond A, Roe BA, Roskin KM, Rubin EM, Rust AG, Santos R, Sapojnikov V, Schultz B, Schultz J, Schwartz MS, Schwartz S, Scott C, Seaman S, Searle S, Sharpe T, Sheridan A, Shownkeen R, Sims S, Singer JB, Slater G, Smit A, Smith DR, Spencer B, Stabenau A, Strange-Thomann NS, Sugnet C, Suyama M, Tesler G, Thompson J, Torrents D, Trevaskis E, Tromp J, Ucla C, Vidal AU, Vinson JP, von Niederhausern AC, Wade CM, Wall M, Weber RJ, Weiss RB, Wendl MC, West AP, Wetterstrand K, Wheeler R, Whelan S, Wierzbowski J, Willey D, Williams S, Wilson RK, Winter E, Worley KC, Wyman D, Yang S, Yang SP, Zdobnov EM, Zody MC, Lander ES. Initial sequencing and comparative analysis of the mouse genome. *Nature* 2002;420:520–562.
2. Nadeau JH, Balling R, Barsh G, Beier D, Brown SDM, Bucan M, Camper S, Carlson G, Copeland N, Eppig J, Fletcher C, Frankel WN, Ganten D, Goldowitz D, Goodnow C, Guenet JL, Hicks G, de Angelis MH, Jackson I, Jacob HJ, Jenkins N, Johnson D, Justice M, Kay S, Kingsley D, Lehrach H, Magnuson T, Meisler M, Poustka AM, Rinchik EM, Rossant J, Russell LB, Schimenti J, Shiroishi T, Skarnes WC, Soriano P, Stanford W, Takahashi JS, Wurst W, Zimmer A. Functional annotation of mouse genome sequences. *Science* 2001;291:1251–1255.

3. de Angelis MH, Flaswinkel H, Fuchs H, Rathkolb B, Soewarto D, Marschall S, Heffner S, Pargent W, Wuensch K, Jung M, Reis A, Richter T, Alessandrini F, Jakob T, Fuchs E, Kolb H, Kremmer E, Schaeble K, Rollinski B, Roscher A, Peters C, Meitinger T, Strom T, Steckler T, Holsboer F, Klopstock T, Gekeler F, Schindewolf C, Jung T, Avraham K, Behrendt H, Ring J, Zimmer A, Schughart K, Pfeffer K, Wolf E, Balling R. Genome-wide, large-scale production of mutant mice by ENU mutagenesis. *Nat Genet* 2000;25:444–447.
4. Bock NA, Konyer NB, Henkelman RM. Multiple-mouse MRI. *Magn Reson Med* 2003;49:158–167.
5. Kovacevic N, Henderson JT, Chan E, Lifshitz N, Bishop J, Evans AC, Henkelman RM, Chen XJ. A 3D MRI atlas of the mouse brain with estimates of the average and variability. *Cereb Cortex* 2005;15:639–645.
6. Szczesny G, Veihelmann A, Massberg S, Nolte D, Messmer K. Long-term anaesthesia using inhalatory isoflurane in different strains of mice—the haemodynamic effects. *Lab Anim* 2004;38:64–69.
7. Hennig J, Nauerth A, Friedburg H. RARE imaging: a fast imaging method for clinical MR. *Magn Reson Med* 1986;3:823–833.
8. Maki JH, Johnson GA, Cofer GP, Macfall JR. SNR improvement in NMR microscopy using DEFT. *J Magn Reson* 1988;80:482–492.
9. Busse R, Riederer S, Fletcher J, Bharucha A, Brandt K. Interactive fast spin-echo imaging. *Magn Reson Med* 2000;44:339–348.
10. Hennig J. Multiecho imaging sequences with low refocusing flip angles. *J Magn Reson* 1988;78:397–407.
11. Hennig J, Scheffler K. Easy improvement of signal-to-noise in RARE-sequences with low refocusing flip angles. *Magn Reson Med* 2000;44:983–985.
12. Woessner DE. Effects of diffusion in nuclear magnetic resonance spin-echo experiments. *J Chem Phys* 1961;34:2057–2061.
13. Levitt MH, Freeman R. NMR population-inversion using a composite pulse. *J Magn Reson* 1979;33:473–476.
14. Levitt MH, Freeman R. Compensation for pulse imperfections in NMR spin-echo experiments. *J Magn Reson* 1981;43:65–80.
15. Shaka AJ, Freeman R. Composite pulses with dual compensation. *J Magn Reson* 1983;55:487–493.
16. Poon CS, Henkelman RM. 180° refocusing pulses which are insensitive to static and radiofrequency field inhomogeneity. *J Magn Reson* 1992;99:45–55.
17. Zhou YQ, Davidson L, Henkelman RM, Nieman BJ, Foster FS, Yu LS, Chen XJ. Ultrasound-guided left-ventricular catheterization: a novel method of whole mouse perfusion for microimaging. *Lab Invest* 2004;84:385–389.
18. Dazai J, Bock NA, Nieman BJ, Davidson LM, Henkelman RM, Chen XJ. Multiple mouse biological loading and monitoring system for MRI. *Magn Reson Med* 2004;52:709–715.
19. Guilfoyle DN, Dyakin VV, O’Shea J, Pell GS, Helpert JA. Quantitative measurements of proton spin-lattice (T1) and spin-spin (T2) relaxation times in the mouse brain at 7.0 T. *Magn Reson Med* 2003;49:576–580.
20. Dockery SE, Suddarth SA, Johnson GA. Relaxation measurements at 300 MHz using MR microscopy. *Magn Reson Med* 1989;11:182–192.
21. Just M, Thelen M. Tissue characterization with T1, T2, and proton density values: results in 160 patients with brain tumors. *Radiology* 1988;169:779–785.
22. Foster MA, Hutchison JMS. Practical NMR imaging. Oxford: IRL Press; 1987. p 40.
23. Poon CS, Henkelman RM. Robust refocusing pulses of limited power. *J Magn Reson A* 1995;116:161–180.
24. Sled JG, Pike GB. Correction for B1 and B0 variations in quantitative T2 measurements using MRI. *Magn Reson Med* 2000;43:589–593.
25. Madore B, Henkelman RM. Motion artifacts in fast spin-echo imaging. *J Magn Reson Imaging* 1994;4:577–584.
26. Olson EM, Bergin CJ, King MA. Fast SE MRI of the chest: parameter optimization and comparison with conventional SE imaging. *J Comp Assist Tomogr* 1995;19:167–175.
27. Wood ML, Henkelman RM. The magnetic field dependence of the breathing artifact. *Magn Reson Med* 1986;4:387–392.
28. Wood ML, Henkelman RM. Suppression of respiratory motion artifacts in magnetic resonance imaging. *Med Phys* 1986;13:794–805.
29. Hinks RS, Constable RT. Gradient moment nulling in fast spin-echo. *Magn Reson Med* 1994;32:698–706.
30. Weismann F, Ruff J, Hiller K-H, Rommel E, Haase A, Neubauer S. Developmental changes of cardiac function and mass assessed with MRI in neonatal, juvenile and adult mice. *Am J Physiol Heart Circ Physiol* 2000;278:H652–H657.
31. Weismann F, Szimtenings M, Frydrychowicz A, Illinger R, Hunecke A, Rommel E, Neubauer S, Haase A. High-resolution MRI with cardiac and respiratory gating allows for accurate *in vivo* atherosclerotic plaque visualization in the murine aortic arch. *Magn Reson Med* 2003;50:69–74.